Filamentary probe on the COMPASS tokamak

K. Kovarik,[1,2,a)] I. Duran,[1] J. Stockel,[1] J. Seidl,[1] J. Adamek,[1] M. Spolaore,[3] N. Vianello,[3] P. Hacek,[1,2] M. Hron,[1] and R. Panek[1]
[1]*Institute of Plasma Physics of the CAS, Za Slovankou 3, Prague 182 00, Czech Republic*
[2]*Faculty of Mathematics and Physics, Charles University, Ke Karlovu 3, Prague 121 16, Czech Republic*
[3]*Consorzio RFX (CNR, ENEA, INFN, Università di Padova, Acciaierie Venete SpA), Corso Stati Uniti 4, 35127 Padova, Italy*

(Received 19 December 2016; accepted 10 February 2017; published online 8 March 2017)

This paper describes a new filamentary probe recently introduced on the COMPASS tokamak. It allows the measurement of electrostatic and magnetic properties of the filaments and their changes in dependence on distance from the separatrix in the region between a divertor and midplane. The probe head is mounted on a manipulator moving the probe radially on a shot-to-shot basis. This configuration is suitable for the long term statistical measurement of the plasma filaments and the measurement of their evolution during their propagation from the separatrix to the wall. The basics of the filamentary probe construction, the evolution of the plasma parameters, and first conditional averages of the plasma filaments in the scrape-off layer of the COMPASS tokamak during the L-mode regime are presented. [http://dx.doi.org/10.1063/1.4977591]

I. INTRODUCTION

Due to their characteristic shape, plasma structures elongated along the magnetic field lines within the scrape-off layer (SOL) are called plasma filaments. Filaments have increased density and temperature in comparison to the background plasma[1–3] and move radially outwards from the plasma column due to $\vec{E}\times\vec{B}$ forces. Electric current conducted along the filaments was observed on the RFX-mod and ASDEX-U.[4,5] Higher plasma density and temperature and carried electric current increase carried energy. Thus, the plasma filaments increase energy and particle transport within the SOL from plasma to the walls. This carried energy is deposited on the vessel walls and in-vessel components very unequally and represents a seriosus danger for these parts. Particularly, groups of filaments during the H-mode known as ELMs are representing severe danger for the first wall and divertor components as well as inserted diagnostics and instrumentation.[6,7] This work presents a recently introduced combined diagnostic system for the measurement of the plasma filaments' electromagnetic features located in an unusual position between the midplane and divertor on the COMPASS tokamak.[8] Moreover, we confirm the presence of the parallel electric current flowing along the filament within the SOL in the L-mode. We have analysed mutual dependencies of filament properties. In Sec. III, we present parameters of the conditionally averaged plasma filaments during the L-mode regime, particularly carried parallel current density j_{par}, ion saturation current I_{sat}, and floating potential V_{float} and their dependence on the distance to the separatrix r_{sep}.

A. Plasma filaments

Plasma filaments are turbulent structures appearing in all magnetic confinement devices within all magnetic topologies, e.g., on the RFX-mod,[9] CASTOR,[10] TJ–II,[11] TCV,[12] MAST,[13] etc. They are released from the confinement region as a cloud of hot and dense plasma. This cloud starts to propagate in the confinement region and after passing the separatrix they continue in a movement away from the separatrix and poloidally according to the $\vec{E}\times\vec{B}$ force.[14] The typical size of the filaments is in the order of centimetres in the direction perpendicular to magnetic field lines. Typical velocities are in the order of km/s in the direction perpendicular to the magnetic field lines.[15,16]

Numerical models usually calculate the self-consistent local evolution of electron density n_e, electron and ion temperature T_e and T_i, plasma potential Φ, vorticity ω (e.g., ESEL), and in some cases parallel electric current density j_{par} (e.g., TOKAM3X, SOLF1D).[17–19] But the measurement of all listed properties, in order to validate these codes, with good enough spatial and temporal resolution is almost impossible. Moreover, electrostatic measurements are usually performed using midplane manipulators and/or divertor probes. Other locations are observed with optic diagnostics that can confirm shape and speed of the filament but not the plasma parameters. Moreover, only a few devices introduced probes allowing the measurement of the magnetic properties of the filaments, i.e., electric currents along the filament. Therefore, the output of the codes is usually validated on electrostatic parameters for the midplane region and/or the divertor region if calculated.

We decided to focus on the magnetic features of the plasma filaments in the L-mode. Thus, we prepared a new diagnostic probe that contains not only Langmuir tips for the filament identification and basic analysis but the system of coils as well. It allows the investigation of magnetic features of the filaments and, namely, the parallel electric current flowing alongside the filament.

II. FILAMENTARY PROBE

The primary goal of the probe is the measurement of the parallel electric current within the plasma structures within

a)Electronic mail: kovarik@ipp.cas.cz

the SOL. A probe with similar goal was already operated at the RFX-mod in Padova;[4] therefore, we cooperated with the team in the development of the probe for the COMPASS tokamak. The sample probe from the RFX-mod was optimized for the detailed measurement of the filament cross section and minimum effect on filaments. Therefore, the RFX-mod probe covers large space of $r \times p = 50 \times 160$ mm with a gap of 88 mm between the towers. Our probe was optimized for tokamak conditions with a higher ratio of toroidal and poloidal components of magnetic field ($B_T/B_{pol} \sim 5$ at the COMPASS tokamak and $B_T/B_{pol} \sim 1$ on the RFX-mod) and made more compact to reduce the impact on plasma with maximized gap between the towers to minimize the effect on the plasma filaments.

Calculation of the parallel current requires the sequence of points with the measurement of poloidal and radial magnetic fields enclosing the area where the plasma filament is passing. We solved this issue by placing 3 sets of 3D coil systems in the radial direction into two identical poloidally separated towers. The coils (their centres, respectively) enclose a space of 18×44 mm and the free space between towers is 20 mm wide, see Fig. 1. The space between the towers is a compromise between the minimized probe impacts on passing filaments (the distance between towers is comparable to the filament poloidal size), keeping a small distance between the measuring coils to minimize the spatial effect for the parallel current calculation and total outer dimensions of the probe head to allow insertion into the access port with a diameter of 100 mm.

The detection of the filaments is performed by a set of Langmuir tips located identically on each tower. Triplet at the top of the probe is used to observe the parameters of the plasma and the possible risk of probe damage assessment. The tips are in an array in the poloidal direction and separated by 4 mm. The second block of the Langmuir tips forms the so-called rake probe.[20] It consists of 6 L tips in a radial array located on the side oriented towards the midplane and it is used for the detection of the filaments (namely, the tower B with Langmuir tips located on the inner side) and for the detailed analysis of the filament electrostatic parameters and the assessment of their radial speed using their correlation. The tips are separated by 4 mm and a cover range of 20 mm. It should be highlighted that the radii covered by the rake probe correspond to the radii covered by the coil systems.

A photograph of the final probe head is in Fig. 1 together with the schematic drawing of its position within the poloidal cut of the COMPASS tokamak with a highlighted separatrix during the flat-top phase of a standard discharge #8118.

The towers are made of boron nitride as one of a few materials that is vacuum compatible electric insulator with a high temperature limit and good heat conductivity. Thermal properties are important for probe survival in the tokamak plasma in the SOL in a reasonable distance from the separatrix. The thickness of the boron-nitride walls of the probe head is at least 5 mm due to the required mechanical strength. Thermal simulation predicted heating up of the probe surface up to 700 °C in case the of electron density of $n_e = 5 \times 10^{18}$ m^{-3} and temperature of T_e = 35 eV that is above the expected parameters in the location of the filamentary probe. An electric insulator is necessary in order to minimize the effect on the filaments including short circuiting in both perpendicular and parallel directions with respect to the magnetic field lines.

The probe is inserted in the tokamak scrape-off layer close to the separatrix below the midplane (port 14/15 AL). It can be positioned up to 20 mm from the separatrix of standard discharge flat-top phase in dependence on probe position and plasma shape and position. Large space between the separatrix, vessel wall, and outer divertor leg allows the insertion of the probe deep into the vessel that ensures that the measurement is not affected by the vessel wall. The mounting of the filamentary probe allows radial movement and angular adjustment on a shot-to-shot basis. Due to its fixed position, the filamentary probe is optimal for the statistical analysis of the SOL turbulent structures. On the other hand, the unusual position in between the midplane and divertor does not allow direct comparison with measurements of probes located at the midplane.

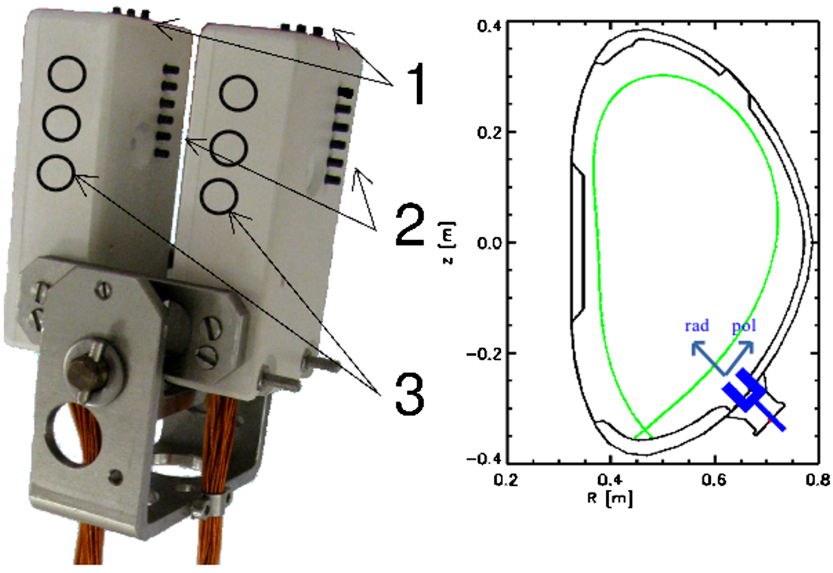

FIG. 1. Left—Photograph of the filamentary probe (1—top probe triplets, 2—rake probes, 3—coil sets hidden inside the probe head) and right—schematic illustration of filamentary probe (blue) position of filamentary probe inside the COMPASS tokamak with indicated poloidal and radial directions (green line represents separatrix position during the flat-top phase of standard discharge #8118).

Radial distances (resolution and ranges) recalculated to the midplane are approximately 60% of the original values with dependence on plasma shape and position and the probe position. Signals from coil sets and Langmuir tips are amplified by dedicated electronics and acquired by a DTACQ216 data acquisition system with sampling rate 5 MSPS.

The observed filaments in the L-mode have time of passage over the probe in the order of 3 μs. Such time scale practically excludes measurement with swept probes as the sweep pass is much longer than filament passage. Therefore, Langmuir tips are used in regimes for the measurement of ion saturation current I_{sat} or floating potential V_{float}. All I_{sat} signals are measured with a biasing voltage of $U_{bias} = -180$ V. This biasing voltage is comparable with the deepest peaks of floating potential of big plasma structures and, therefore, it is not suitable to straightforward plasma density calculation, but it is low enough for plasma filaments' identification with no risk of electric arcs making the signal useless at all. The Langmuir tips of the filamentary probe can be set individually in the I_{sat} or V_{float} regime. During the series of the measurement, we used a probe connection that, according to our opinion, suits for the measurement of the filament properties as well as further statistical measurements within the SOL and might be useful for the development and validation of theoretical models of the SOL plasma behaviour. The connection of the individual channels is as follows:

- the top triplets are connected in the ion saturation current (middle tip) and floating potential (2 edge tips) regime,
- the whole rake probe on the opened side (tower A) is connected in the ion saturation regime in order to obtain clear correlations between the signals,
- the rake probe in between the towers (tower B) is connected alternately in floating potential and ion saturation current regimes starting with floating potential on the tip closest to the separatrix.

Langmuir tips in rake probes in the same regime are used for correlation analysis such as the estimation of filament radial velocity and effective size. Dependent variables as local plasma density and temperature are not calculated as we are not able to measure other variables needed for their evaluation.

The parallel electric current density within the filament can be calculated from signals of magnetic coils using Ampere's integral,

$$\mu_0 I = \oint \vec{B} \cdot \vec{dl}. \tag{1}$$

In our case, it means that a sequence summation of radial and poloidal components of the magnetic field, averaged from coils at the beginning and end of the spatial segment for each time element, multiplied by corresponding distances of the actual coils blocks

$$\mu_0 I = \sum_{A1\text{–}A2\text{–}A3\text{–}B6\text{–}B5\text{–}B4\text{–}A1} \left(\frac{B^i_{rad} + B^{i+1}_{rad}}{2} d_{rad} + \frac{B^i_{pol} + B^{i+1}_{pol}}{2} d_{pol}\right), \tag{2}$$

where d_{rad} or d_{pol} could be zero if the poloidal or radial coordinates of the coil blocks are the same. Coil signals are directly acquired and the signal is integrated numerically to obtain the magnetic field value. Data acquisition starts after the toroidal magnetic field reaches the requested value and approximately 50 ms before the plasma breakdown. Not all the coil blocks from the sequence $A1$–$A2$–$A3$–$B6$–$B5$–$B4$–$A1$ have to be used but the number of used coil blocks reduces the estimate errors. The computed parallel current is divided by the area enclosed by the used coil blocks, see Fig. 2.

The second possible method for parallel current calculation is the Maxwell equation,

$$\mu_0 \vec{j} = rot \vec{B}, \tag{3}$$

where we use 3 blocks of the coils for the calculation of the spatial derivatives of the magnetic field. In particular, we chose 3 coil blocks where 2 of them have the same radial coordinate, e.g., $A1$–$A2$–$B4$ ($r_{A1} = r_{B4}$, highlighted in Fig. 2 with green line). The equation is

$$\mu_0 j_{\parallel} = \frac{B^{A1}_{pol} - B^{A2}_{pol}}{d_{rad}} - \frac{B^{A1}_{rad} - B^{B4}_{rad}}{d_{pol}}. \tag{4}$$

In order to reduce the effects of spatial dependence of the method response, we calculate the average value of all reasonable combinations of the coils for each time element. Effective position of the parallel current density is established as the average of the used coil block's positions.

Results obtained by both methods are similar in shape and values. Due to the effect of the main plasma current on absolute values of reconstructed parallel electric current density, we present only parallel electric current density fluctuations.

The filamentary probe is capable to detect L-mode plasma filaments and measure the evolution of the filament properties as apparent in Fig. 3. The ion saturation current signal of *RakeB2* probe shows clearly the characteristic peak which corresponds to the peak in plasma density as the main feature of the filament (a) that is kept during its movement in the SOL. Therefore, ion saturation current peaks are used for the detection of the presence of the filaments.

The floating potential shows strong perturbation characterized by initial increase and sudden drop (Fig. 3(b)) that is

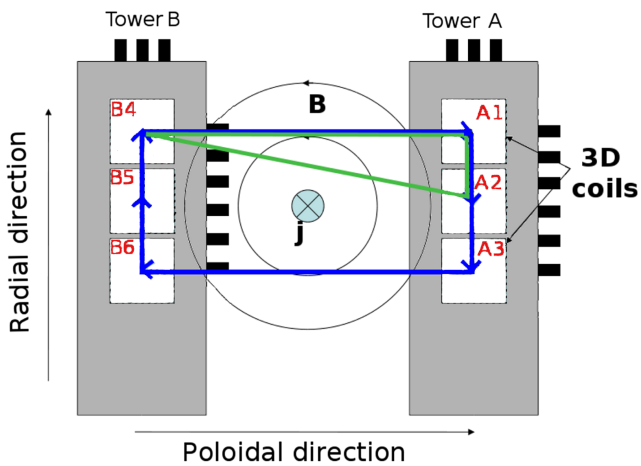

FIG. 2. Illustration of parallel current calculation from filamentary probe magnetic measurements using the Ampere's integral (blue arrows) and method based on the rotB Maxwell equation (green triangle connecting blocks $A1$, $A2$, and $B4$).

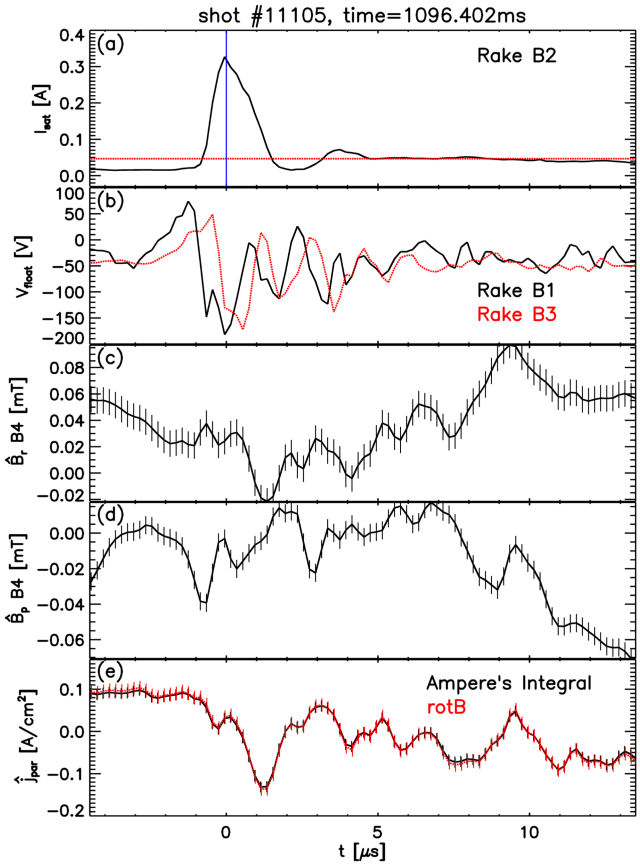

FIG. 3. Signals of I_{sat} with the filament detection level in red (a), V_{float} (b) (tips closer (black) and farther (red) from the separatrix), perturbation of radial magnetic field B_{rad} (c), perturbation of poloidal magnetic field B_{pol} (d), and corresponding calculated fluctuation of j_{par} (e) (black calculated using the Ampere's integral, red with the rotB method) of the L-mode plasma filament (discharge #11105 t = 1096.402 ms).

influenced by changes in the plasma potential and increase of electron temperature within the filament.[21,22] This evolution changes with the potential balance and cooling of the plasma. This change is faster than the change in the density profile. It is visible on signals with a different distance to the separatrix, i.e., a different lifetime of the filament since the release from the plasma. The comparison of signals from Langmuir tips *RakeB*1 (closer to plasma) and *RakeB*3 (farther from plasma) shows decrease in the amplitude of the signal swing that illustrates the graph Fig. 3(b) where the signal of probe *RakeB*3 shows a lower amplitude of the perturbation than the signal *RakeB*1, and similarly, fluctuations of floating potential of the signal *RakeB*3 are in shorter time reduced below a level of ±10 V within a time window of 1 μs.

During the passage of the filament over the filamentary probe was observed the perturbation of magnetic field (Figs. 3(c) and 3(d)). This perturbation corresponds to the change of parallel electric current flowing (Fig. 3(e)). In this case, the parallel current perturbation is shifted in time from the originating filament. It can be the effect of the different position of effective point of parallel current evaluation (the mean value of used coil block positions) with respect to the Langmuir tip *RakeB*2 used for identification or the filament is not passing clearly over the Langmuir tip *RakeB*2 and the detected maximum

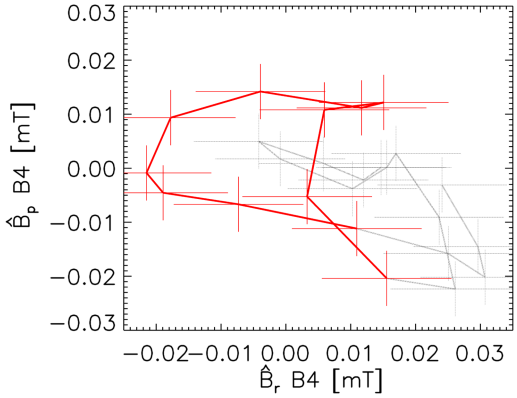

FIG. 4. Hodogram of perpendicular magnetic field fluctuations during the filamentary structure passage over the filamentary probe. Highlighted part represents time of the parallel electric current density perturbation (#11105, t = 1096.402 ms).

of I_{sat} signal does not correspond to the centre of the filament or inhomogeneity of the parallel electric current density distribution over the filament. The continuation of evolution of the magnetic perturbation and consequent parallel electric current density perturbation can be caused by another current filament passing near the filamentary probe out of the range of presented rake probe B.

A hodogram of the magnetic perturbation clearly shows the mutual transition of individual components of the magnetic field, see Fig. 4. Red line highlights the time segment when the parallel current peak appears. It can be seen that the magnetic field transforms from one direction to another and back and, as a consequence, the perturbation forms an enclosed line in the hodogram.

III. COMPARISON AND AVERAGING OF THE FILAMENTARY PROBE DATA

The plasma filaments and their properties change in dependence on many parameters and the comparison of individually measured filaments can be confusing. Therefore, we perform the analysis in 3 steps. At first, we compare the given parameters of individual filaments. At second, we create conditionally averaged signals of the filaments to obtain a representative filament for the given combination of the plasma parameters, shape and distance between the plasma separatrix and the filamentary probe. And finally, we compare the properties of the averaged filaments.

Fortunately, the filamentary probe position and holder construction are optimal for the long term observation of the plasma structures and their averaging due to its fixed position. Detection of the filament and consequent averaging is based on the most significant feature of the filaments, the peak in plasma density appearing as the peak in the ion saturation current signal. In practise, we detect the local maximum of the I_{sat} signal and denote all the parts of the peak above the detection level $I_{sat} - \overline{I_{sat}} \geq A * \sigma$, where σ is the standard deviation, as the sought-after filamentary structure, see Fig. 5. The threshold of detection is usually A = 2.5 to distinguish individual filaments. This allows a clear definition of filament parameters to be compared, e.g., I_{sat} signal amplitude, waiting time

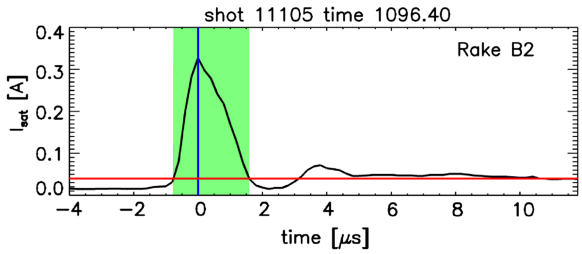

FIG. 5. Principles of L-mode filament detection on I_{sat} signal during the discharge #11105 (t = 1196.402 ms). Local maximum (blue vertical line) and the whole part of the peak (green area) above the detection level (red line $-2.5\ \sigma$) for further analysis is highlighted.

(time since the previous filament), duration of the filament (duration of I_{sat} signal being above detection level), and some characteristics of the individual signals, namely, the swing amplitude (difference of maximum and minimum) of the signal during the filament. Subsequently, we can correlate the signals and evaluate properties with signals such as the filament velocity and effective size (duration of the filament passage multiplied by the filament velocity). We use an additional condition of reliable estimate of radial velocity from near signal correlation reaching at least a value of 0.5. Measured filaments' properties are compared for multiple discharges. In this work, we choose ohmic L-mode discharges #11104–#11108 with similar plasma parameters and shape during the flat-top phase, $B_T = 1.14$ T, $I_P = 200$ kA, $n_e = 5 \times 10^{19}$ m^{-3}, $\kappa = 1.37$, $q_{95} = 3.86$. The filamentary probe remains on the same position during these discharges.

A. Filament properties correlations

One of our goals is the search for the mutual dependence of individual parameters of the filaments on each other. A possible correlation is illustrated by mutual plots of the parameters of individual filaments. In this work, we show the swing amplitude of the parallel electric current density during the filament with the duration of the filament according to the ion saturation current signal and waiting times since the former plasma filament.

The mutual plot of swing amplitude of parallel electric current fluctuation $\hat{j_{par}}$ on the filament duration $t_{filament}$ shows apparent dependence, see Fig. 6. The level of correlation reaches a value of $R2 = 0.596$ for analysed filaments. A similar level of mutual correlation was observed, e.g., I_{sat} amplitude, swing amplitude of $\hat{V_{float}}$, swing amplitude of $\hat{j_{par}}$, and filament duration $t_{filament}$ as well. This correlation suggests mutual dependence between the filament parameters where more compact filaments carry and conserve higher parallel electric current. The broadening of the correlation suggests the influence of more parameters and will be further investigated.

On the other hand, we do not see any correlation between, e.g., the swing amplitude of the parallel electric current density fluctuation $\hat{j_{par}}$ and waiting time of the filament t_{wait}, see Fig. 7. The correlation coefficient is even negative in this case, $R2 = -0.07$. Actually, the waiting time t_{wait} seems to be uncorrelated with any other filament parameters including its duration $t_{filament}$ and I_{sat} amplitude in discharges #11104–#11108.

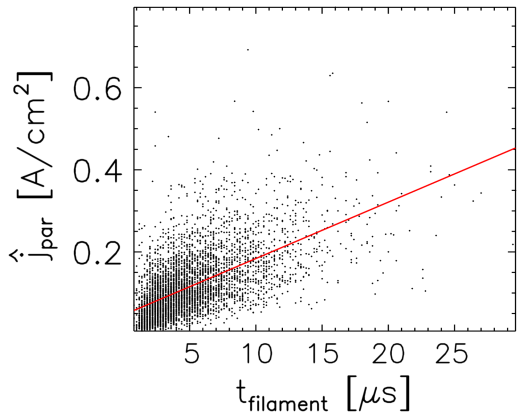

FIG. 6. Swing amplitude of the parallel current density $\hat{j_{par}}$ in dependence on duration of the filament $t_{filament}$ for L-mode discharges #11104–#11108. The suggested linear approximation is given in red.

B. Conditional averages of parameter evolution

Except these significant parameters of the filaments, we compare the evolution of conditionally averaged evolution of signals during the filament. Presented signals are averaged only from individual Langmuir tip or coil block each that avoid the deformation of the result by an incorrect subtraction of the filament drift effect causing the temporal shift of the measured evolution of individual filament.

The evolution of the conditionally averaged L-mode plasma filament is presented in Fig. 8. Chosen filaments were detected using the Langmuir tip *RakeB*2, i.e., on the inner wall of tower B second from top of the probe and first in the ion saturation current regime in this array and deep enough in between the coils to allow a better assignment of magnetic perturbations to the coils (coil block *B*4) and reconstructed parallel electric current to the space between the coils. Averaged signals come from only one diagnostic element each.

The evolution of the ion saturation current (*RakeB*2 and *RakeB*4) is smoothed into a peak characterized by fast exponential growth and slower exponential decrease of the signal (Fig. 8(a)). The characteristic time constants of the signal rise and decrease during the filaments are $\tau_{up} = 13.7\ \mu$s and $\tau_{down} = 37.1\ \mu$s, respectively, for the peak on conditionally averaged signal *RakeB*2 used for detection. The peak density on the probe *RakeB*4 is not only

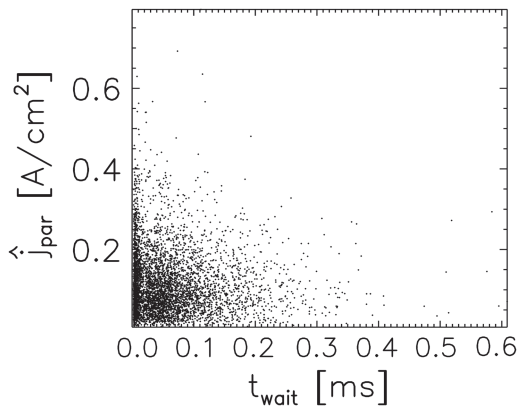

FIG. 7. Swing amplitude of the parallel current density $\hat{j_{par}}$ in dependence on waiting time of the filament t_{wait} for L-mode discharges #11104–#11108.

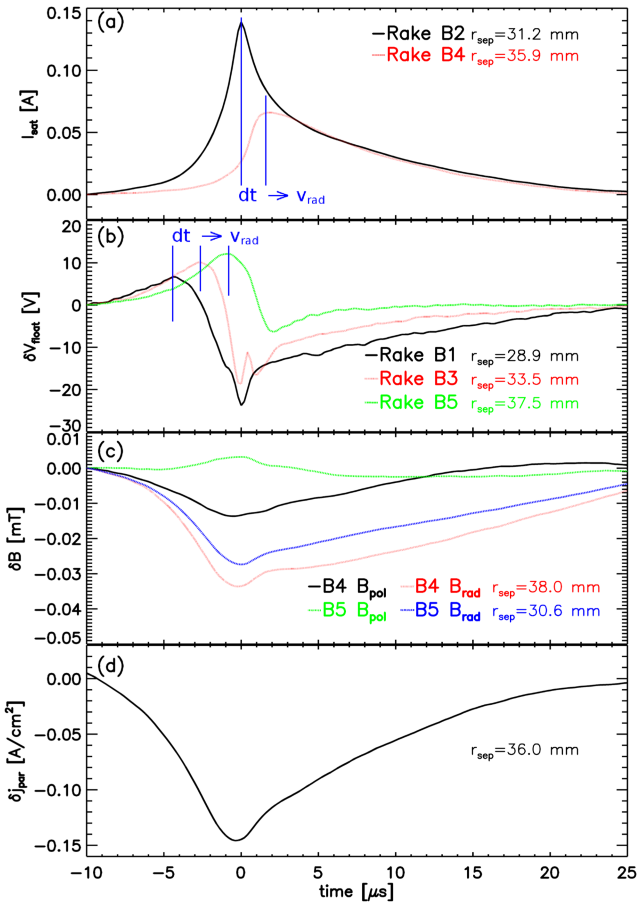

FIG. 8. Evolution of the basic parameters during the conditionally averaged L-mode filament (4832 filaments). Perturbation of ion saturation current δI_{sat} (a), floating potential δV_{float} (b), magnetic field in radial and poloidal directions δB_{rad} and δB_{pol}, respectively (c), and reconstructed parallel electric current density δj_{par} (d). Corresponding distance to the separatrix on midplane r_{sep} is highlighted for each signal.

decreased but temporally blurred as the individual filaments have different velocities. Out of time shift of the peaks, we can assume the radial velocity of the averaged filament as $v_{rad} = 5.4 \pm 2.3$ km/s.

The evolution of the floating potential V_{float} (Fig. 8(b)) shows clearly an increase at the beginning of the filament and drop near the maximum of the I_{sat} signal. Signals of floating potential combine changes in the plasma potential and temperature, particularly the electron temperature. Separation of these effects one from another is not possible with only one not swept probe. The conditional averages of the floating potential signals on *RakeB*1, *RakeB*3, and *RakeB*5 show a clear decrease of the swing of the floating potential with a decay length of $\lambda_{Vfloat} = 39$ mm. Apparent is the time shift of the drop as well. The corresponding radial velocity is $v_{rad} = 5.2 \pm 1.8$ km/s. Differences in the shape of the curves can be caused by several mechanisms. Additionally to the effect of the distance to the separatrix, i.e., different lifetime of the filament, we have to take into account a possible movement of the filament not only radially along the filamentary probe tower but with poloidal component, i.e., temporal evolutions represent different cuts through the filament. The last is the presence of the probe head itself with the effect on cooling of the plasma, recycling, etc. The assessment of the influence level for all these mechanisms will be part of our future work.

Perturbation of magnetic field (Fig. 8(c)) is more significant in the radial component (δB_{rad}—red and blue) than in the poloidal component (δB_{pol}—black and green) of magnetic field. Moreover, the poloidal component of the magnetic perturbation in coil block *B*4 has an opposite direction than in coil block *B*5. Explanation is in mutual positions of the coil blocks *B*4, *B*5 and the Langmuir tip *RakeB*2 used for the detection of the filaments. The Langmuir tip is shifted poloidally in particular and, therefore, the recorded passing filament and its parallel current is poloidally shifted from the coils. The maximum poloidal component can be obtained if the filament passes in front of the tower, i.e., is detected by the Langmuir tips in the triplet on the top of the probe head. The radial position of the Langmuir tip *RakeB*2 is in the middle between the coil blocks *B*4 and *B*5 and implies that the source of perturbation for poloidal coils of blocks *B*4 and *B*5 is on the opposite side from the coil axis and, therefore, the signals have opposite direction. The absence of time shift between the signals is again in the triggering of the event in the same time when the centre of the filament is close to the detecting Langmuir tip *RakeB*2 and not moving over the probes.

The perturbation of parallel electric current (Fig. 8(d)) follows the trend of radial magnetic field perturbation with strong broad peak close to the peak of ion saturation current. This suggests the correlation of the parallel current density with the plasma density within the filament, similarly to Fig. 6. A similar correlation was observed on the RFX-mod[3] with similar amplitudes of parallel electric current perturbation j_{par} in the order of kA/m^2 the RFX-mod, i.e., similar as on the COMPASS tokamak.

In future, we will continue with the statistical analysis of filaments' properties and their dependencies for L-mode, ELMs, and inter-ELM phases. We expect, namely, higher parallel electric current in ELMs as promising from the comparison of magnetic perturbation of ELMs (30 mT) and L-mode filaments (0.1 mT) on the RFX-mod.[4,5] The increase is expected to be approximately 2 orders of magnitude. Some preliminary results are shown in Ref. 23.

IV. CONCLUSIONS

We have put in operation a special combined probe head allowing the measurement of electromagnetic properties of the plasma filaments within the scrape-off layer of the COMPASS tokamak. Temporal and spatial resolution satisfies to observe the temporal evolution of the passing L-mode filaments and their spatial structure. The probe allows a clear measurement of the plasma filament parameters including the parallel electric current perturbation.

Localisation and fixed position of the filamentary probe is optimal for the statistical analysis of the passing filamentary structures. We have found correlations of significant properties of the filaments, namely, between the swing amplitude of parallel electric current density $\hat{j_{par}}$, swing amplitude of floating potential $\hat{V_{float}}$, ion saturation current amplitude I_{sat}, and duration of the L-mode filament $t_{filament}$. These correlations will be

further analysed in other discharges. No correlation was found with the waiting time of the L-mode filaments t_{wait}.

We have presented the conditionally averaged evolution of the filamentary probe signals and discussed its features and dependence on the distance to the separatrix. The basic properties of the conditionally averaged filaments confirm most of the expected behaviour of the individual plasma filaments. A deep interpretation of the filamentary probe data on broader database of filaments is needed for a clear understanding of the filament physics and will be performed in future. We will continue with the statistical analysis of filaments' properties and their dependencies for L-mode, ELMs, and inter-ELM phases.

ACKNOWLEDGMENTS

This work has been carried out within the framework of the EUROfusion Consortium and has received funding from the Euratom research and training programme 2014-2018 under Grant Agreement No. 633053, co-funded by Ministry of Education, Youth and Sports Project No. 8D15001, and Czech Science Foundation Nos. GA15-10723S and GA16-25074. The views and opinions expressed herein do not necessarily reflect those of the European Commission.

[1] S. I. Krasheninnikov, "On scrape off layer plasma transport," Phys. Lett. A **283**, 368 (2001).
[2] J. Boedo, "Transport by intermittent convection in the boundary of the DIII-D tokamak," Phys. Plasmas **8**, 826 (2001).
[3] M. Spolaore, N. Vianello, M. Agostini, R. Cavazzana, E. Martines, P. Scarin, G. Serianni, E. Spada, M. Zuin, and V. Antoni, "Direct measurements of current filament structures in magnetic-confinement fusion device," Phys. Rev. Lett. **102**, 165001 (2009).
[4] M. Spolaore, N. Vianello, M. Agostini, R. Cavazzana, E. Martines, G. Serianni, P. Scarin, E. Spada, M. Zuin, and V. Antoni, "Magnetic and electrostatic structures measured in the edge region of the RFX-mod experiment," J. Nucl. Mater. **390-391**, 448 (2009).
[5] E. Martines, N. Vianello, D. Sundkvist, M. Spolaore, M. Zuin, M. Agostini, V. Antoni, R. Cavazzana, C. Ionita, M. Maraschek, F. Mehlmann, H.-W. Muller, V. Naulin, J. J. Rasmussen, V. Rohde, P. Scarin, R. Schrittwieser, G. Serianni, E. Spada, and RFX-Mod Team and ASDEX Upgrade Team, "Current filaments in turbulent magnetized plasmas," Plasma Phys. Controlled Fusion **51**, 124053 (2009).
[6] A. Loarte, G. Saibene, R. Sartori, D. Campbell, M. Becoulet, L. Horton, T. Eich, A. Herrmann, G. Matthews, N. Asakura, A. Chankin, A. Leonard, G. Porter, G. Federici, G. Janeschitz, M. Shimada, and M. Sugihara, "Characteristics of type I ELM energy and particle losses in existing devices and their extrapolation to ITER," Plasma Phys. Controlled Fusion **45**, 1549 (2003).
[7] J. Adamek, J. Seidl, M. Komm, V. Weinzettl, R. Panek, J. Stckel, M. Hron, P. Hacek, M. Imrisek, P. Vondracek, J. Horacek, A. Devitre, and COMPASS Team, "Fast measurements of the electron temperature and parallel heat flux in ELMy H-mode on the COMPASS tokamak," Nucl. Fusion **57**, 022010 (2017).
[8] R. Panek *et al.*, "Status of the COMPASS tokamak and characterization of the first H-mode," Plasma Phys. Controlled Fusion **58**, 014015 (2016).
[9] M. Spolaore, V. Antoni, E. Spada, H. Bergsaker, R. Cavazzana, J. R. Drake, E. Martines, G. Regnoli, G. Serianni, and N. Vianello, "Coherent structure diffusivity in the edge region of Reversed Field Pinch experiments," J. Phys.: Conf. Ser. **7**, 253 (2005).
[10] J. Stockel, J. Badalec, I. Duran, M. Hron, J. Horacek, K. Jakubka, L. Kryska, J. Petrzilka, F. Zacek, M. V. P. Heller, Z. A. Brazilio, and I. L. Caldas, "Magnetic and electrostatic fluctuations in the CASTOR tokamak," Plasma Phys. Controlled Fusion **41**, A577 (1999).
[11] M. Spolaore, N. Vianello, I. Furno, D. Carralero, M. Agostini, J. A. Alonso, F. Avino, R. Cavazzana, G. De Masi, A. Fasoli, C. Hidalgo, E. Martines, B. Momo, A. Scaggion, P. Scarin, S. Spagnolo, G. Spizzo, C. Theiler, and M. Zuin, "Electromagnetic turbulent structures: A ubiquitous feature of the edge region of toroidal plasma configurations," Phys. Plasmas **22**, 012310 (2015).
[12] O. E. Garcia, R. A. Pitts, J. Horacek, A. H. Nielsen, W. Fundamenski, J. P. Graves, V. Naulin, and J. Juul Rasmussen, "Turbulent transport in the TCV SOL," J. Nucl. Mater. **363**, 575 (2007).
[13] A. Kirk, T. Eich, A. Herrmann, H.-W. Muller, L. D. Horton, G. F. Counsell, M. Price, V. Rohde, V. Bobkov, B. Kurzan, J. Neuhauser, H. Wilson, and ASDEX Upgrade and MAST Team, "The spatial structure of type-I ELMs at the mid-plane in ASDEX Upgrade and a comparison with data from MAST," Plasma Phys. Controlled Fusion **47**, 995 (2005).
[14] D. A. D'Ippolito, J. R. Myra, and S. J. Zweben, Phys. Plasmas **18**, 060501 (2011).
[15] A. Kirk, A. Herrmann, B. Ayed, T. Eich, H. W. Muller, G. F. Counsell, S. Lisgo, M. Price, A. Schmid, S. Tallents, and H. Wilson, "Comparison of the filament behaviour observed during type I ELMs in ASDEX Upgrade and MAST," J. Phys.: Conf. Ser. **123**, 012012 (2008).
[16] A. Theodorsen, O. E. Garcia, J. Horacek, R. Kube, and R. A. Pitts, "Scrape-off layer turbulence in TCV: Evidence in support of stochastic modelling," Plasma Phys. Controlled Fusion **58**, 044006 (2016).
[17] E. Havlickova *et al.*, "Steady-state and time-dependent modelling of parallel transport in the scrape-off layer," Plasma Phys. Controlled Fusion **53**, 065004 (2011).
[18] J. R. Angus, M. V. Umansky, and S. I. Krashenninikov, "Review and limitations of 3D plasma blob modeling with reduced collisional fluid equations," J. Nucl. Mater. **438**, S572 (2013).
[19] P. Tamain, H. Bufferand, G. Ciraolo, C. Colin, D. Galassi, Ph. Ghendrih, F. Schwander, and E. Serre, "The TOKAM3X code for edge turbulence fluid simulations of tokamak plasmas in versatile magnetic geometries," J. Comput. Phys. **321**, 606 (2016).
[20] J. Stockel, J. Adamek, P. Balan, O. Bilyk, J. Brotankova, R. Dejarnac, P. Devynck, I. Duran, J. P. Gunn, M. Hron, J. Horacek, C. Ionita, M. Kocan, E. Martines, R. Panek, P. Peleman, R. Schrittwieser, G. Van Oost, and F. Zacek, "Advanced probes for edge plasma diagnostics on the CASTOR tokamak," J. Phys.: Conf. Ser. **63**, 012001 (2007).
[21] J. Horacek, J. Adamek, H.-W. Muller, J. Seidl, A. H. Nielsen, V. Rohde, F. Mehlmann, C. Ionita, E. Havlickova, and ASDEX Upgrade Team, "Interpretation of fast measurements of plasma potential, temperature and density in SOL of ASDEX Upgrade," Nucl. Fusion **50**, 105001 (2010).
[22] O. E. Garcia, J. Horacek, R. A. Pitts, A. H. Nielsen, W. Fundamenski, V. Naulin, and J. Juul Rasmussen, "Fluctuations and transport in the TCV scrape–off layer," Nucl. Fusion **47**, 667 (2007).
[23] M. Spolaore, K. Kovarik, J. Stockel, J. Adamek, R. Dejarnac, I. Duran, M. Komm, T. Markovic, E. Martines, R. Panek, J. Seidl, N. Vianello, and COMPASS Team, "Electromagnetic ELM and inter-ELM filaments detected in the COMPASS Scrape-Off Layer," Nucl. Mater. Energy (published online 2016).